

TCS Overview and Vacuum System Upgrade

*Kenneth Miller, Houyang Guo, Alan Hoffman, Adam Pietrzyk
Redmond Plasma Physics Lab, University of Washington*

Abstract

The rotating magnetic field (RMF) has been shown to be very effective in driving toroidal currents in normal flux confined prolate FRCs. Both the FRC's driven current and poloidal flux will increase until the torque exerted on the electrons by the RMF is balanced by the torque due to electron-ion friction. The FRC will expand radially (adjusting axially according to energy and particle balance), compressing the external flux and increasing the density and azimuthal current, until the applied torque is balanced by the resistive drag. The relative RMF penetration is proportional to the fraction of the total number of electrons involved in the current drive process (driven near synchronously with the RMF), and it will adjust itself such that the driven current will fully reverse the external field. It is a fundamental feature of the RMF drive process that this occurs automatically as long as there are sufficient electrons to carry the azimuthal current, without all being driven synchronously.

This basic torque balance sets the relation between the density, the RMF field amplitude, the fraction of the electrons involved in the current drive process, and the plasma resistivity. However, it does not impose a hard constraint on either the external field, or the total temperature, which are related to the density through radial pressure balance. Since the total temperature appears to have been limited in past experiments by strong impurity ingestion and subsequent radiation after the initial formation phase, the confining external field was also limited. Measurements suggest that oxygen was the primary contaminant, as in other unbaked, non wall conditioned systems.

A major upgrade of the TCS vacuum chamber is presently underway to address the impurity issue and thus allow higher temperature and field operation. All o-rings will be removed and heating blankets will be installed to bake the system to 200 °C. Tantalum clad internal flux rings will be installed to shield the quartz vacuum wall (which is necessary to allow RMF penetration) from the plasma. Cleaning and wall conditioning will be performed with a glow discharge and boronization and/or titanium gettering. Operation at temperatures and fields beyond those set by the radiative temperature barrier should allow an assessment of the intrinsic energy loss processes associated with RMF FRC sustainment.

Introduction:

The RMF is a transverse rotating magnetic field that is used to form and sustain the FRC, [figure 1](#). It penetrates a distance Δr into the plasma, [figure 2](#), and exerts a torque on the electrons, $T_{\text{RMF}} = 2\pi B_{\omega}^2 r_s^2 I_{\text{ant}}(\Delta r/r_s)/\mu_0$. This applied torque is countered by the torque due to electron-ion resistivity, $T_{\eta} = 0.5\pi e^2 \eta_{\perp} r_s^4 \langle n_e^2 \omega_e \rangle I_{\text{FRC}}$. In equilibrium, these two torques balance each other and the RMF penetrates just far enough to maintain the FRC's diamagnetic current. The governing relationship between the RMF and the plasma then becomes $n_e \sim B_{\omega}/(\eta_{\perp} \omega_{\text{RMF}} r_s^2)^{0.5}$, a relationship which is seen experimentally as well, [figure 3](#).

The growth or decay of the FRC is governed by the azimuthal electric field at the FRC's null, E_{θ} , which is set by the difference between the RMF drive torque and the resistive torque, $d\phi_p/dt = 2\pi R E_{\theta(r=R)} = 2(T_{\text{RMF}} - T_{\eta})/n_e e r_s^2 I_s$. E_{θ} also arises in Ohm's Law, of which the azimuthal component is $E_{\theta} = \eta_{\perp} j_{\theta} - \langle v_{ez} B_r \rangle + v_{er} B_z - v_{ez} B_r$, where $\eta_{\perp} j_{\theta}$ is the resistive drag, $\langle v_{ez} B_r \rangle$ is the RMF drive term, and $v_{er} B_z$ and $v_{ez} B_r$ are flow terms that propagate the RMF drive to regions where it has not penetrated, typically inside the null and at the FRC ends when the FRC is longer than the RMF antenna, [figure 4](#) and [figure 5](#). In the RMF drive term, v_{ez} is the oscillatory 'screening' current driven by the RMF and B_r is the r component of the applied RMF, whereas in the flow terms, v_{ez} is the outward diffusion of plasma at the FRC ends and B_r is the radial component of the FRC's poloidal flux as it wraps around.

Traces illustrative of TCS operation are shown in [figure 6](#), and corresponding radial profiles are shown in [figure 7](#). The RMF is turned on at $t = 0$, and it rapidly drives enough current to form an FRC,

typically forming one in 100 μsec to 200 μsec . At around 350 μsec , both the density and impurity radiation rapidly increase as the plasma becomes aware of the wall and material liberated from it due to its presence. Consequently, both the temperature and edge field fall. After around 700 μsec , an equilibrium is reached that is largely set by the recycling rate of deuterium and impurities off the vacuum walls.

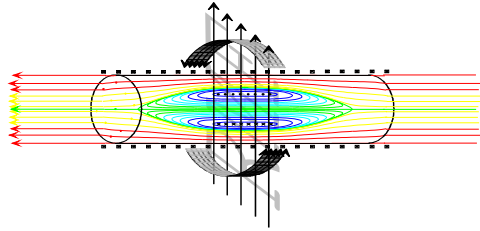


Figure 1. Schematic of the RMF applied to the FRC. The FRC is a current ring and associated closed field held by an external axial field. Pure plasma pressure at the null balances the edge magnetic pressure.

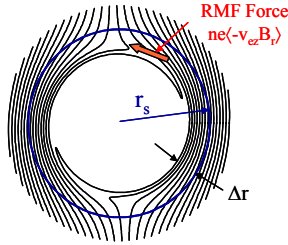


Figure 2. Cross section showing a partially penetrated RMF. Δr is the RMF penetration depth and r_s is the plasmas separatrix radius.

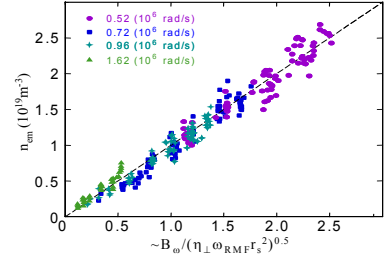


Figure 3. Observation of the scaling of n_e with $B_\omega / (\eta_\perp \omega_{RMF} r_s^2)^{0.5}$, as anticipated from the analytic expressions of torque balance.

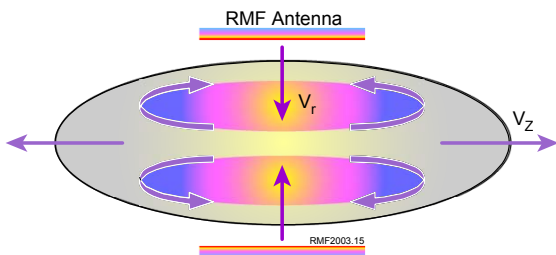


Figure 4. Cartoon of the expected flow patterns in an RMF driven FRC. The flow consists of two basic components: a closed circulating flow, and a flow where particles are driven in from the plasma's sides and then diffuse axially out its ends.

$$E_\theta = \eta_\perp j_\theta + \langle -\tilde{v}_{ez} \tilde{B}_r \rangle + V_r B_z - V_z B_r$$

Under Antenna

Outer: -

+

-

+

Inner: -

+

-

+

FRC Ends

Outer: -

+

-

+

Inner: -

+

-

+

Figure 5. How and where each term in Ohm's Law contributes to the overall RMF drive process. A '-' sign indicates drag while a '+' sign indicates drive.

Impurity radiation:

In equilibrium, when the RMF drive torque is balanced by resistive drag, the RMF imposes a constraint on the plasma density, $n_e \sim B_\omega / (\eta_\perp \omega_{RMF} r_s^2)^{0.5}$, **figure 3**. The constraint of radial pressure balance relates the edge magnetic pressure B_e to the plasma pressure at the null, $B_e = (2\mu_0 n_e kT)^{0.5}$. Since n_e is fixed by the RMF, B_e and T must vary together. Thus, if T is clamped, say by radiation, then B_e is also clamped.

Though visible in **figure 6**, this behavior is better illustrated in **figure 8**, another typical pulse that does not undergo the rapid jump in the density at around 350 μsec . The top two traces show how B_e and T scale together. When T is high, so is B_e . The third trace shows the rise of the radiated power from the plasma. Initially, when this radiated power is small, T is high, but as the radiated power rises, T falls. The time scale of the rise in radiated power is similar to that of the plasma particle confinement time. It is also similar to the time it takes CIII levels to return to their normal level when operating with CD_4 doped deuterium. The fourth trace shows how the OIII line radiation mimics the total radiated power. Based on the inability to see any difference in the oxygen line radiation when oxygen doped deuterium is used, except for very early in time, it is suspected that oxygen is the primary contaminant, a suspicion which is consistent with the use of unconditioned stainless steel in the vacuum vessel.

Radiation is the dominant power loss mechanism, as shown in figure 9. The line indicates where the total radiated power would correspond to 100% of the input power. The color on the data points corresponds to the RMF frequency of operation. There are some experimental indications that a scaling of the plasma resistivity with the ratio of B_w/B_e compounds the above problem. The clamp on T , and thus B_e induces operation at higher ratios of B_w/B_e . If this increases η , then n_e will fall, further reducing B_e . The plasma resistivity is measured to be lower when operating at smaller ratios of B_w/B_e , though there is still certainly some discussion as to which causes which.

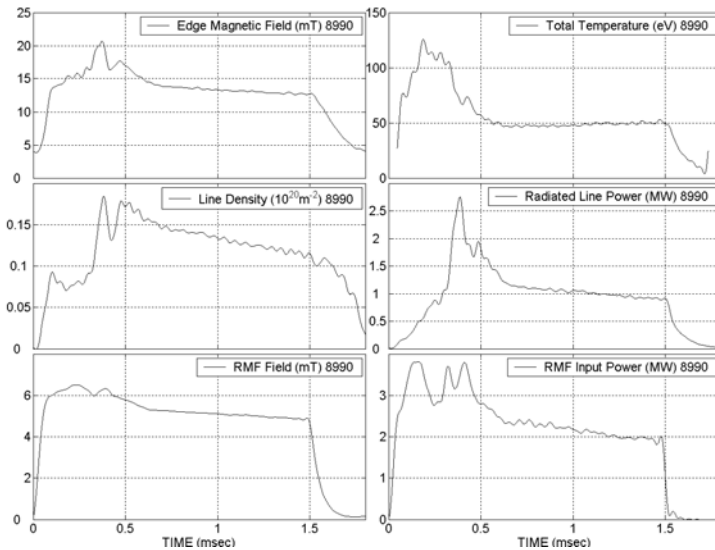


Figure 6. Traces typical of TCS operation at mid RMF frequency, 114 kHz

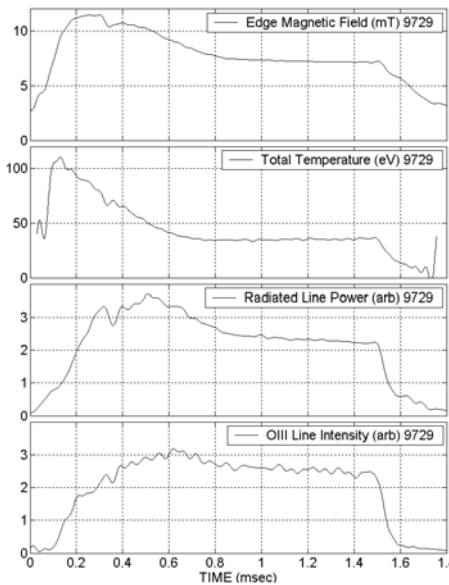


Figure 8. Traces showing the correlation between B_e and T , T and the radiated power, and the radiated power and the OIII line intensity

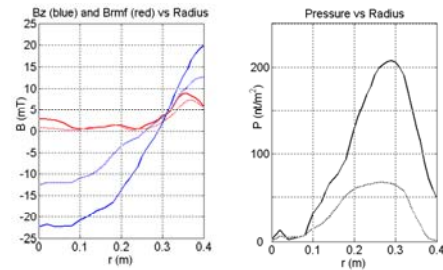


Figure 7. The two graphs above show radial magnetic and pressure profiles. The solid lines correspond to $t = 400 \mu\text{sec}$, while the dotted lines correspond to $t = 1400 \mu\text{sec}$. Quite surprisingly, even though the RMF current drive is sustained, the RMF barely penetrates to the null. The very low RMF amplitude at the null implies a correspondingly low plasma resistivity there, since at the null, the RMF drive term is the only term that counters plasma resistivity. Numeric modeling is presently being done to study the implications of a non uniform plasma resistivity.

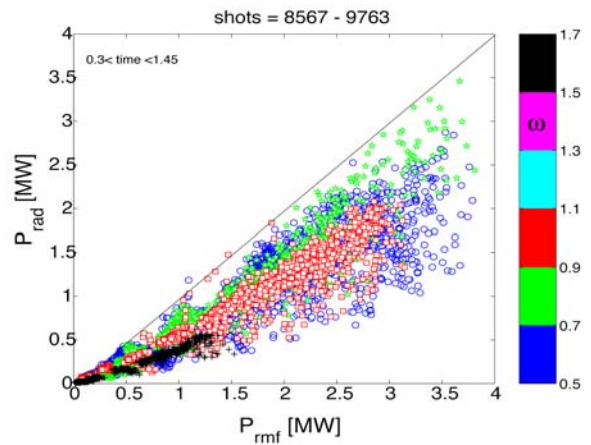


Figure 9. Radiated Power vs Total Input Power

TCS vacuum system upgrade:

A major upgrade of the TCS vacuum chamber is presently underway to address the impurity issue and thus allow higher temperature and field operation. A scale schematic of the machine upgraded is shown in [figure 10](#). Significant improvements will include the following:

- All o-rings will be removed so that the entire system can be baked. The target temperature is 200 °C. In the metal to metal joints, metal c-rings will be used. The seal to the quartz tube will be made to metal bellows adhered to the quartz with a very high temperature, low out gassing, and low mass loss epoxy. The bellows will be made from Invar to minimize stresses on the quartz caused by different coefficients of thermal expansion.
- A glow discharge system, along with Titanium gettering and/or Boronization ((CH₃)₃B), will be employed.
- Internal tantalum clad flux rings (L/R ~ 6 msec) will be placed over the quartz confinement section to protect the quartz from the plasma.
- A tantalum shield will be placed over the inside of both end cones. A tantalum cone placed over one of the existing cones has proven to be highly effective.
- The two transition sections will be enlarged from a 27 cm I.D. to a 48 cm I.D. to facilitate transport of conventionally formed FRCs from the LSX/mod source section without wall contact. These conventionally formed plasmas have exhibited unusually low resistivities, and they could make ideal target plasmas for the RMF.
- Additional ports will be provided, particularly in the end cones, to allow study of regions outside of the FRC midplane.

Presently, the vacuum system design is nearly complete, and the magnets and some large vacuum components are out for bids. The most challenging piece of the upgrade, the quartz section of the vacuum chamber that sits under the RMF antenna, is under construction. It is being made by adding support ribs and ports to one of our existing quartz tubes. The existing tubes are reinforced with epoxy impregnated kevlar bands to hold vacuum, but they would likely fail at the target system bake out temperature of 200 °C. Quartz is being used since it is essential to have an insulating section in the vacuum chamber to allow the RMF in. We considered placing the RMF antennas inside the vacuum chamber, but were concerned about arcing and other adverse plasma interactions given the high voltages applied.

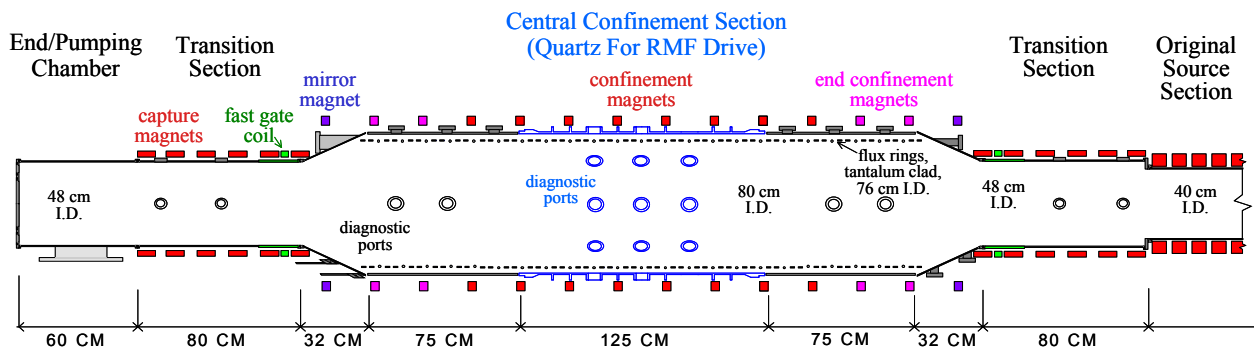


[Figure 10](#). Scale schematic of TCS vacuum system upgrade.

Summary:

The rotating magnetic field has been shown to be very effective in driving toroidal currents in normal flux confined prolate FRCs. The balance between the RMF drive torque and the plasma

resistive drag determines the plasma density, $n_e \sim B_\omega / (\eta_\perp \omega_{\text{RMF}} r_s^2)^{0.5}$, Radial pressure balance relates T and B_e to n_e , $B_e = (2\mu_0 n_e kT)^{0.5}$. For a given n_e , B_e and T scale together. T appears to be clamped by impurity radiation, probably oxygen, and because of this B_e is also clamped. A major upgrade of the TCS vacuum chamber is presently underway to address the impurity issue and thus allow higher temperature and field operation. Operation at temperatures and fields beyond those set by the radiative temperature barrier should allow an assessment of the intrinsic energy loss processes associated with RMF FRC sustainment.